

## State-selective spectroscopy of water up to its first dissociation limit

Maxim Grechko,<sup>1</sup> Oleg V. Boyarkin,<sup>1,a)</sup> Thomas R. Rizzo,<sup>1</sup> Pavlo Maksyutenko,<sup>1</sup> Nikolay F. Zobov,<sup>2</sup> Sergei V. Shirin,<sup>2</sup> Lorenzo Lodi,<sup>3</sup> Jonathan Tennyson,<sup>3</sup> Attila G. Császár,<sup>4</sup> and Oleg L. Polyansky<sup>2,3</sup>

<sup>1</sup>Laboratoire de Chimie Physique Moléculaire (LCPM), École Polytechnique Fédérale de Lausanne, Lausanne CH-1015, Switzerland

<sup>2</sup>Institute of Applied Physics, Russian Academy of Sciences, 46 Uljanov Street, Nizhny Novgorod 603950, Russia

<sup>3</sup>Department of Physics and Astronomy, University College London, London WC1E 6BT, United Kingdom

<sup>4</sup>Institute of Chemistry, Laboratory of Molecular Spectroscopy, Loránd Eötvös University, P.O. Box 32, H-1518 Budapest 112, Hungary

(Received 13 September 2009; accepted 20 November 2009; published online 14 December 2009)

A joint experimental and first-principles quantum chemical study of the vibration-rotation states of the water molecule up to its first dissociation limit is presented. Triple-resonance, quantum state-selective spectroscopy is used to probe the entire ladder of water's stretching vibrations up to 19 quanta of OH stretch, the last stretching state below dissociation. A new ground state potential energy surface of water is calculated using a large basis set and an all-electron, multireference configuration interaction procedure, which is augmented by relativistic corrections and fitted to a flexible functional form appropriate for a dissociating system. Variational nuclear motion calculations on this surface are used to give vibrational assignments. A total of 44 new vibrational states and 366 rotation-vibration energy levels are characterized; these span the region from 35 508 to 41 126  $\text{cm}^{-1}$  above the vibrational ground state. © 2009 American Institute of Physics. [doi:10.1063/1.3273207]

Water is arguably the most important polyatomic molecule in the universe; for example, its rotation-vibration spectrum largely controls both the absorption of sunlight and the greenhouse effect on earth. The dense spectrum of hot water has been observed in sunspots<sup>1</sup> and was the first to be recorded in an extrasolar planet.<sup>2</sup> Water is a benchmark system for first-principles quantum mechanical treatments<sup>3</sup> and novel experimental procedures.<sup>4,5</sup>

Direct access to high vibrational levels just below the dissociation by a single photon has negligibly weak absorption. Ultralong path length, single-photon experiments have probed the spectrum of water into the near ultraviolet<sup>6</sup> leading to the excitation of vibrational states with up to eight quanta of OH stretch. Previous two-photon studies by us<sup>7,8</sup> assigned rotation-vibration states of water up to 35 000  $\text{cm}^{-1}$  above the vibrational ground state of water; these states included vibrations with up to 12 quanta of OH stretch. Recently we used a state-selective, triple-resonance experimental protocol to obtain a significantly improved dissociation energy of water,  $D_0 = 41\,145.94 \pm 0.15 \text{ cm}^{-1}$ .<sup>9</sup> Here this procedure is adapted to probe and assign individual states from the 12th OH stretch level up to the lowest dissociation limit on the electronic ground state surface of water. The experiments provide access to nuclear motion states up to the first dissociation threshold via three sequential OH stretch overtone transitions between single rotational levels (see Fig. 1), excited by three laser pulses of 5–7 ns duration. In this triple-resonance overtone excitation scheme a photon from the first

laser (P1) promotes a fraction of the water vapor molecules in a chosen rotational state to a level that contains four vibrational quanta in one of the stretches. A photon of the second laser (P2) promotes up to half of these pre-excited molecules to a second intermediate level that corresponds to either eight or nine quanta of OH stretch, the gateway state. A third photon (P3) further excites molecules from the gate-

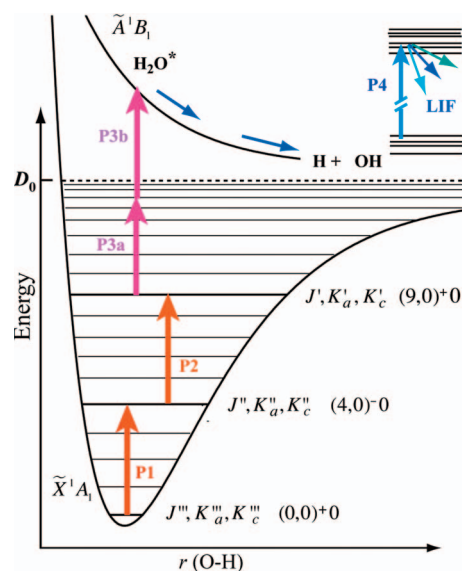


FIG. 1. Schematic energy level diagram and excitation scheme employed in experiments. The states are labeled by the asymmetric top rotational quantum numbers ( $J, K_a, K_c$ ) and by the three vibrational quantum numbers  $(m, n)^+ - v_2$  in local mode notation (Ref. 18), where  $m$  and  $n$  are the quantum numbers for stretching vibrations and  $v_2$  is the bending quantum number.

<sup>a)</sup>Author to whom correspondence should be addressed. Electronic mail: oleg.boiarkin@epfl.ch.

way state to a state below the dissociation threshold. This three-step excitation scheme allows an increase in the overall fraction of molecules promoted to the terminal vibrational level by many orders of magnitude compared to a hypothetical single excitation by a UV laser field of a similar fluence. Spectral selectivity is given by the rigorous selection rules that govern the change in rotational angular momentum  $J$  ( $\Delta J=0, \pm 1$ ), its projection onto the laboratory  $z$ -axis and the parity for each transition. Because rotational relaxation in our experiments is suppressed by using low pressure (50  $\mu$ bar) and short delays (10 ns) between the excitation laser pulses, the known rotational identity of the originating and the intermediate states in conjunction with the selection rules leaves only a few options for rotational assignment of the final rovibrational states. Moreover, in certain cases changing relative directions of linear polarizations of the last two overtone lasers allows us to control the rotational quantum number  $J$  of the molecules in the upper terminal states. This gives an additional means of verification of the state assignment. The total energy of a terminal state is determined as the sum of the known energy of the starting level<sup>10</sup> and the energies of the three excitation photons. Wave numbers of all the lasers have been simultaneously monitored by a high precision wave meter, assuring  $\pm 0.03$   $\text{cm}^{-1}$  absolute accuracy in the determination of the total excitation energy.

Water molecules in the terminal rovibrational level are promoted to the repulsive  $\tilde{A}^1B_1$  electronic state by a second photon from the third excitation laser, yielding OH and H fragments. We subsequently detect OH in the ground state ( $X^2\Pi_{3/2}, e, J=\frac{3}{2}, v=0$ ) via laser-induced fluorescence using a fourth laser pulse. To increase detection efficiency we allow some collisional relaxation of the appearing hot OH fragments by introducing 100 ns delay between the last excitation (P3) and the detection (P4) photons. Monitoring OH fluorescence as a function of the wave number of the third laser pulse in the sequence, while keeping the wave numbers of all other lasers fixed, generates a photofragment excitation spectrum. Such an action spectrum truly reflects wave numbers of transitions, but the detection scheme may distort their relative intensities. Altogether we measured the energies of 366 levels, which are tabulated in Ref. 11. These levels come from 44 different vibrational bands whose band origins, which lie from 35 500  $\text{cm}^{-1}$  all the way up to dissociation, are given in Table I. The assigned rotational states have quantum number  $J$  ranging between 0 and 7.

Understanding the observed spectra requires the execution of sophisticated electronic structure and nuclear motion computations. Here, unlike earlier, lower-energy studies,<sup>7,8</sup> we use an entirely *ab initio* procedure to model the spectrum up to dissociation. The electronic structure computations used in this study employed the atom-centered, aug-cc-pCV6Z Gaussian-type orbital basis from the correlation-consistent family.<sup>12</sup> Electronic wave functions were determined at the internally contracted multireference configuration interaction (IC-MRCI) level with a renormalized Davidson correction (+Q) using the MOLPRO package.<sup>13</sup> All electrons were considered during the correlation treatment. The carefully chosen, large reference space used included all the eight valence electrons of water and ten mo-

TABLE I. Vibrational band origins for highly excited states of water.

Assignment <sup>a</sup> ( $m, n$ ) <sup>+/-</sup> $v_2$	Band origin/ $\text{cm}^{-1}$		
	Observed <sup>b</sup>	Calculated	(Obs-Calc)
(11, 1) <sup>+</sup> 0	35 509 <sup>c</sup>	35 515.61	-7.0
(11, 1) <sup>-</sup> 0	35 509.68	35 516.87	-7.2
(13, 0) <sup>+</sup> 0	35 585.96	35 591.83	-5.9
(13, 0) <sup>-</sup> 0	35 586.01	35 592.38	-6.4
(12, 0) <sup>+</sup> 2	36 179.32	36 185.49	-6.2
(12, 0) <sup>-</sup> 2	36 180 <sup>c</sup>	36 185.83	-6.0
(13, 0) <sup>+</sup> 1	36 684.05	36 687.95	-3.9
(13, 0) <sup>-</sup> 1	36 684.88	36 688.88	-4.0
(11, 1) <sup>+</sup> 1	36 740.60	36 745.61	-5.0
(11, 1) <sup>-</sup> 1	36 739.78	36 745.28	-5.5
(14, 0) <sup>+</sup> 0	37 122.70	37 122.23	0.5
(14, 0) <sup>-</sup> 0	37 122.72	37 122.20	0.5
(12, 1) <sup>+</sup> 0	37 439 <sup>c</sup>	37 437.54	1.0
(12, 1) <sup>-</sup> 0	37 439 <sup>c</sup>	37 437.54	1.0
(13, 0) <sup>+</sup> 2	37 765.65	37 767.32	-1.7
(13, 0) <sup>-</sup> 2	37 766 <sup>c</sup>	37 767.31	-2.0
(14, 0) <sup>+</sup> 1	38 153.25	38 149.88	3.4
(14, 0) <sup>-</sup> 1	38 153.31	38 149.92	3.4
(15, 0) <sup>+</sup> 0	38 462.52	38 453.58	8.9
(15, 0) <sup>-</sup> 0	38 462.54	38 453.58	9.0
(14, 0) <sup>+</sup> 2	39 123.77	39 118.56	5.2
(14, 0) <sup>-</sup> 2	39 124 <sup>c</sup>	39 118.54	5.0
(15, 0) <sup>+</sup> 1	39 390.26	39 375.60	14.7
(15, 0) <sup>-</sup> 1	39 390.22	39 375.60	14.6
(16, 0) <sup>+</sup> 0	39 574.55	39 553.99	20.6
(16, 0) <sup>-</sup> 0	39 574.54	39 554.00	20.5
(13, 1) <sup>+</sup> 1	40 044.57	40 022.77	21.8
(13, 1) <sup>-</sup> 1	40 044.72	40 022.72	22.0
(15, 0) <sup>+</sup> 2	40 226 <sup>c</sup>	40 211.82	14.0
(15, 0) <sup>-</sup> 2	40 226.31	40 212.24	14.1
(16, 0) <sup>+</sup> 1	40 370.55	40 342.29	28.3
(16, 0) <sup>-</sup> 1	40 370.83	40 342.62	28.2
(17, 0) <sup>+</sup> 0	40 437.23	40 405.23	32.0
(17, 0) <sup>-</sup> 0	40 437.26	40 405.39	31.9
(14, 1) <sup>+</sup> 0	40 708 <sup>c</sup>	40 698.08	10.0
(14, 1) <sup>-</sup> 0	40 707.77	40 697.98	9.8
(18, 0) <sup>+</sup> 0	40 947.43	40 888.94	58.6
(18, 0) <sup>-</sup> 0	40 949.31	40 887.28	62.0
(17, 0) <sup>+</sup> 1	40 984.64	40 960.20	24.4
(17, 0) <sup>-</sup> 1	40 982.89	40 959.14	23.8
(19, 0) <sup>+</sup> 0	41 101.34	41 056.25	45.1
(19, 0) <sup>-</sup> 0	41 103.66	41 055.82	47.8
(16, 0) <sup>+</sup> 2	41 122.69	41 082.69	40.0
(16, 0) <sup>-</sup> 2	41 125.22	41 082.76	42.5

<sup>a</sup>Local mode notation (see Fig. 1 captions for details).

<sup>b</sup>Experimental accuracy  $\pm 0.03$   $\text{cm}^{-1}$ .

<sup>c</sup>Extrapolated from levels with  $J > 0$ .

lecular orbitals of ( $A', A''$ )=(8, 2) symmetry. This choice, which extends our previous reference space, was based on analysis of earlier results,<sup>3,14,15</sup> on comparison with full configuration interaction (FCI) results using the cc-pVDZ basis set, and comparison of equilibrium dipoles with accurate coupled cluster with singles, doubles, triples and quadruples (CCSDTQ) results. The IC-MRCI+Q/aug-cc-pCV6Z computations were carried out at 2200 geometries yielding a global potential energy surface (PES) for the electronic ground state of water correctly sampled up to the first dissociation

limit. The energy values, with relativistic corrections calculated as the sum of one-electron mass-velocity and Darwin terms, were fitted to a flexible functional form.<sup>16</sup> The resulting surface gives  $D_0=41\,108\text{ cm}^{-1}$ ,  $38\text{ cm}^{-1}$  lower than the measurement.<sup>9</sup> A FORTRAN program giving this potential is supplied in Ref. 11.

A number of variational nuclear motion calculations have considered vibrational or rotational-vibrational states of water up to its first dissociation limit.<sup>17–19</sup> Here nuclear motion calculations were performed on our new potential with an augmented version of the DVR3D program suite.<sup>20</sup> Calculations were performed in Radau coordinates, with a bisector embedding for states with  $J>0$ , and used previously optimized Morse oscillatorlike functions.<sup>8</sup> The angular motions were represented by 38 (associated-)Legendre functions. The final vibrational matrix had a dimension of  $15\,000 \times 15\,000$ . For rotationally excited states, 1500 functions for each  $k$  value were retained from DVR3DRJZ and used as the basis set for ROTLEV3B.<sup>19</sup> These calculations converged energy levels to better than  $1\text{ cm}^{-1}$ . Transition intensities from the gateway state are computed using the core-valence-relativistic (CVR) dipole moment surface, modified to give correct asymptotic behavior. All calculations were performed on a 64-bit Linux workstation with 16 GB of random access memory.

Previous studies<sup>16–18</sup> suggested that the vibrational states of water become highly irregular with little underlying structure. However, the measured spectra are strongly structured with a relatively small number of very strong lines. These observations are mirrored by our calculations, which similarly find series of regular vibrational states associated with local mode stretching states, which extend all the way to dissociation. This suggests that our new potential is qualitatively different in the near dissociation region to those used in previous studies.

Spectral lines were analyzed covering the region between  $35\,000\text{ cm}^{-1}$  and dissociation in a number of regions. Figure 2 gives a typical example of the comparison between the observed and simulated spectra. In making assignments extensive use was made of the systemic trends in the (observed-calculated) transition frequencies as well as the comparison with calculated line strengths. In many cases the rotational quantum number of a particular state could be confirmed experimentally by the use of different gateway states and known selection rules. A full list of assigned transitions and newly determined rotation-vibration energy levels is given in the EPAPS supplementary data.<sup>11</sup> Table I presents the newly determined vibrational band origins, which span energies up to just below dissociation. The assignment of a large number of stretching states and many states with bending excitation up to  $v_2=2$  allows the accuracy of the *ab initio* spectrum to be calibrated. The agreement between theory and experiment is remarkable. The discrepancies between observed and calculated rotationless ( $J=0$ ) vibrational energy levels increase systematically with degree of stretching excitation and are less than  $10\text{ cm}^{-1}$  for energies as high as  $39\,000\text{ cm}^{-1}$  (Table I); discrepancies for excited rotational states are stable and practically equal to those of the corresponding vibrational state with  $J=0$ .

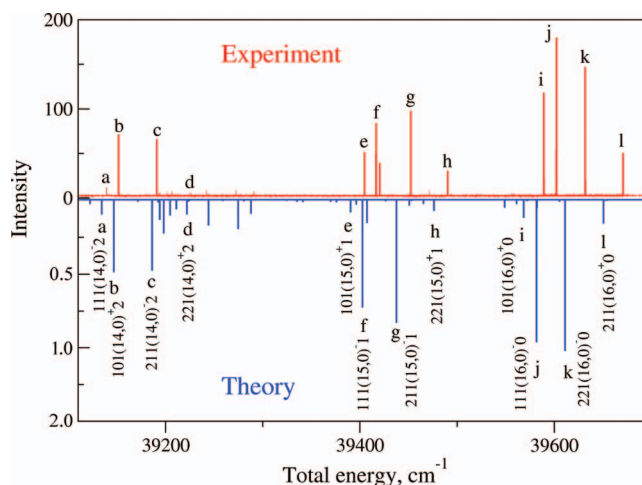


FIG. 2. Triple-resonance spectrum of water from the gateway state prepared via the following pathway:  $[25\,154.61\text{ cm}^{-1}, 110(80)^+0] \leftarrow [13\,864.28\text{ cm}^{-1}, 111(40)^-0] \leftarrow [79.496\text{ cm}^{-1}, 212(00)0]$ . The intensity of observed transitions (upper trace) is given in arbitrary units, while the intensity of calculated transitions (lower trace) is in  $10^{-20}\text{ cm}^2/\text{molecule}$ , assuming unit occupancy of the gateway state. Letters relate observed and calculated transitions. The combination of laser polarization and selection rules results in final states with  $J=1$  or  $2$ . The notation for the final states is the same as used in Fig. 1.

All states with high stretching excitation are quasidegenerate, as anticipated by local mode theory.<sup>21,22</sup> This local mode degeneracy is very pronounced; the calculated energies may coincide to eight digits. However, this degeneracy is partially removed when one of the stretching doublets is perturbed by a neighboring state. All the assigned vibrational states from  $35\,000\text{ cm}^{-1}$  to dissociation appear as local mode doublets; plots are near identical for the even and odd vibrational wave functions.

The results presented above and the benchmark *ab initio* calculation of  $D_0$  by Ruscic *et al.*<sup>23</sup> can be used to provide pointers on how to further improve our potential. The  $D_0$  dissociation energy of the present *ab initio* PES, built on all-electron IC-MRCI+Q/aug-cc-pCV6Z computed energies with relativistic corrections, differs from the well-established experimental value quoted in this article by only  $38\text{ cm}^{-1}$ . This seemingly excellent agreement should not make us forget that there are at least four main “effects” not considered. First, the aug-cc-pCV6Z electronic basis set used, while rather large by today’s standards, carries an incompleteness error due to its finite size. No basis set extrapolation procedure to the complete basis set limit was attempted. We estimate that the correction to  $D_0$  due to basis set incompleteness may be as much as  $80\text{ cm}^{-1}$ . Second, the computation of the correlation energy is based on IC-MRCI; this introduces an error with respect to FCI which, as several observations made during this study suggest, could be as large as  $40\text{--}50\text{ cm}^{-1}$ . This is also the approximate scatter between IC-MRCI-like methods which use different size extensivity corrections (IC-MRCI+Q, IC-MRCI+Pople, IC-ACPF, and IC-AQCC) at energies around  $40\,000\text{ cm}^{-1}$ . Furthermore, using the cc-pVDZ basis, which allows going to the FCI limit, the error of IC-MRCI+Q using the active space is of the order of  $40\text{ cm}^{-1}$ . Third, though scalar relativistic effects calculated as expectation values of the mass-velocity and

one-electron Darwin operators were included in the calculations, these do not account for all such effects. In particular, the effect of spin-orbit interaction on  $D_0$  was reported by Ruscic *et al.*<sup>23</sup> as  $-38 \text{ cm}^{-1}$ . Fourth, the treatment employed does not go beyond the Born–Oppenheimer separation of nuclear and electronic degrees of freedom. An improvement in the accuracy of the *ab initio* calculations could be made by inclusion of adiabatic and nonadiabatic non-Born–Oppenheimer corrections. The adiabatic correction contributes about  $+40 \text{ cm}^{-1}$  to the dissociation energy.<sup>23</sup> The nonadiabatic contribution is difficult to estimate and thus it is not attempted here. Thus, even at the very high level of electronic structure theory employed in this study, it seems that we are gaining accuracy from a fortuitous cancellation of some of the effects not taken into account. Further advance in the *ab initio* computation of the vibrational band origins of water would benefit only from a joint consideration of all these factors as individual inclusion of any one of them might even make some of our predictions worse. A possibility we have yet to pursue is to use our extremely accurate experimental energies to produce a semiempirical potential surface.

In summary, we have demonstrated that selective quantum state spectroscopy, when combined with accurate variational nuclear motion computations, provides a detailed probe of the rovibrational energy level structure of water all the way to its first dissociation limit. It is possible to extend both the theoretical<sup>24</sup> and experimental procedures to probe the region directly above the dissociation limit. Work in this direction is currently in progress in our laboratories.

O.V.B. and T.R.R. thank EPFL and FNS (Grant Nos. 020-112071 and 021-117929) for support. This work was supported by the Russian Fund for Basic Research (Grant No. 09-02-00053), EPSRC, NERC, OTKA, the QUASAAR network, and the Royal Society; S.V.S. thanks RFP (Grant No. MK-1155.2008.2).

<sup>1</sup>O. L. Polyansky, N. F. Zobov, S. Viti, J. Tennyson, P. F. Bernath, and L. Wallace, *Science* **277**, 346 (1997).

<sup>2</sup>G. Tinetti, A. Vidal-Madjar, M.-C. Liang, J.-P. Beaulieu, Y. Yung, S.

- Carey, R. J. Barber, J. Tennyson, I. Ribas, N. Allard, G. E. Ballester, D. K. Sing, and F. Selsis, *Nature (London)* **448**, 169 (2007).
- <sup>3</sup>O. L. Polyansky, A. G. Császár, S. V. Shirin, N. F. Zobov, P. Barletta, J. Tennyson, D. W. Schwenke, and P. J. Knowles, *Science* **299**, 539 (2003).
- <sup>4</sup>R. L. Vanderwal and F. F. Crim, *J. Phys. Chem.* **93**, 5331 (1989).
- <sup>5</sup>A. Callegari, P. Theule, R. N. Tolchenov, N. F. Zobov, O. L. Polyansky, J. Tennyson, J. S. Muentner, and T. R. Rizzo, *Science* **297**, 993 (2002).
- <sup>6</sup>P. Dupré, T. Germain, N. F. Zobov, R. N. Tolchenov, and J. Tennyson, *J. Chem. Phys.* **123**, 154307 (2005).
- <sup>7</sup>P. Maksyutenko, J. S. Muentner, N. F. Zobov, S. V. Shirin, O. L. Polyansky, T. R. Rizzo, and O. V. Boyarkin, *J. Chem. Phys.* **126**, 241101 (2007).
- <sup>8</sup>M. Grechko, P. Maksyutenko, N. F. Zobov, S. V. Shirin, O. L. Polyansky, T. R. Rizzo, and O. V. Boyarkin, *J. Phys. Chem. A* **112**, 10539 (2008).
- <sup>9</sup>P. Maksyutenko, T. R. Rizzo, and O. V. Boyarkin, *J. Chem. Phys.* **125**, 181101 (2006).
- <sup>10</sup>J. Tennyson, N. F. Zobov, R. Williamson, O. L. Polyansky, and P. F. Bernath, *J. Phys. Chem. Ref. Data* **30**, 735 (2001).
- <sup>11</sup>See EPAPS supplementary material at <http://dx.doi.org/10.1063/1.3273207> for (a) for the potential energy surface as a FORTRAN program; (b) a list of measured transition frequencies; and (c) a tabulation of the experimental rotation-vibration energy levels derived from this work.
- <sup>12</sup>The basis set we designate as aug-cc-pCV6Z was obtained through the EMSL basis set exchange web site at <https://bse.pnl.gov/bse/portal>. For H, we use the standard aug-cc-pV6Z basis. For O, the aug-cc-pV6Z part is also standard and the “C” (core-correlation functions) is available on the website as “cc-pCV6Z(old)” and cited as A. K. Wilson and T. H. Dunning, Jr. (to be published). We note that the same website gives a newer “cc-pCV6Z” version whose core functions differ slightly.
- <sup>13</sup>H.-J. Werner, P. J. Knowles, R. Lindh, F. R. Manby, M. Schütz *et al.*, <http://www.molpro.net>.
- <sup>14</sup>P. Barletta, S. V. Shirin, N. F. Zobov, O. L. Polyansky, J. Tennyson, E. F. Valeev, and A. G. Császár, *J. Chem. Phys.* **125**, 204307 (2006).
- <sup>15</sup>L. Lodi, R. N. Tolchenov, J. Tennyson, A. E. Lynas-Gray, S. V. Shirin, N. F. Zobov, O. L. Polyansky, A. G. Császár, J. van Stralen, and L. Visscher, *J. Chem. Phys.* **128**, 044304 (2008).
- <sup>16</sup>L. Lodi, O. L. Polyansky, and J. Tennyson, *Mol. Phys.* **106**, 1267 (2008).
- <sup>17</sup>H. Y. Mussa and J. Tennyson, *J. Chem. Phys.* **109**, 10885 (1998).
- <sup>18</sup>S. K. Gray and E. M. Goldfield, *J. Phys. Chem.* **105**, 2634 (2001).
- <sup>19</sup>G. H. Li and H. Guo, *J. Mol. Spectrosc.* **210**, 90 (2001).
- <sup>20</sup>J. Tennyson, M. A. Kostin, P. Barletta, G. J. Harris, O. L. Polyansky, J. Ramanlal, and N. F. Zobov, *Comput. Phys. Commun.* **163**, 85 (2004).
- <sup>21</sup>M. S. Child and R. T. Lawton, *Chem. Phys. Lett.* **87**, 217 (1982).
- <sup>22</sup>L. Halonen, *Adv. Chem. Phys.* **104**, 41 (1998).
- <sup>23</sup>B. Ruscic, A. F. Wagner, L. B. Harding, R. L. Asher, D. Feller, D. A. Dixon, K. A. Peterson, Y. Song, X. Qian, C. Y. Ng, J. Liu, W. Chen, and D. W. Schwenke, *J. Phys. Chem.* **106**, 2727 (2002).
- <sup>24</sup>B. C. Silva, P. Barletta, J. J. Munro, and J. Tennyson, *J. Chem. Phys.* **128**, 244312 (2008).